CZASOPISMO TECHNICZNE M
WYDAWNICTWO POLITECHNIKI KRAKOWSKIEJ

z. 5-M/2008
ISSN 0011-4561
ISSN 1897-6328

JERZY BAŁDYGA, WOJCIECH ORCIUCH, ANDRZEJ KRASIŃSKI*

APPLICATION OF POPULATION BALANCES TO STUDY COMPLEX PARTICULATE PROCESSES

WYKORZYSTANIE BILANSU POPULACJI W BADANIACH ZŁOŻONYCH PROCESÓW FORMUŁOWANIA NANOZAWIESIN

Abstract

Shear flows of particulate suspensions are investigated for the effect of particle clustering on viscosity using aggregation, breakage and restructuring models for effective viscosity of the suspension and CFD simulation. A complex model based on suspension structure and employing the QMOM population balance modeling is formulated for aggregates consisting of primary nano-particles. Results of numerical simulations are presented for turbulent flows including generation of turbulence and flow laminarization. The *k-ε* and LES models of turbulence were applied. The model has universal character and can be used to any system of three-dimensional geometry including that of practical importance – see an example of the rotor-stator mixer.

Keywords: aggregation, CFD, deagglomeration, population balance, suspension rheology

Streszczenie

Przepływy zagregowanych zawiesin obserwowane są w wielu zastosowaniach technicznych, stanowią też interesujące wyzwanie badawcze ze względu na fakt, że struktura przepływu i generowane naprężenia burzliwe zależą od struktury zawiesiny, struktura zagregowanej zawiesiny zależy od rozmiarów, stężenia i struktury agregatów, zaś rozmiary i struktura agregatów zależą od naprężeń burzliwych i struktury przepływu. Wymienione współzależności opisano, korzystając z CFD, bilansu populacji i modelu konstytutywnego wiążącego lepkość zawiesiny z jej strukturą. Podano przykładowe wyniki symulacji, łącznie z tymi o znaczeniu praktycznym.

Słowa kluczowe: agregacja, CFD, deaglomeracja, bilans populacji, reologia zawiesin

* Prof. Jerzy Bałdyga, dr Wojciech Orciuch, dr Andrzej Krasiński,
Wydział Inżynierii Chemicznej i Procesowej, Politechnika Warszawska.

1. Introduction

Balancing of populations and theoretical approaches that make possible description of state and dynamics of a population of any considered entities may be regarded as classical problems of statistical mechanics that were defined and solved more than a hundred years ago by Liouville and Boltzmann [1], whereas fundamentals for methods of treating populations of aggregating particles were introduced by Smoluchowski [2] in 1917.

The Liouville equation is in the form of equation of continuity in the 6N phase space (a specific space or Γ-space). Namely, in order to describe the varying states of all the particles present in the considered system one can use the phase space with separate coordinates (3 for momentum, 3 for the position) assigned to each particle, so that all of them are the space axes. Then the Liouville equation takes the form

$$\left(\frac{\partial}{\partial t}+\sum_{i=1}^{N}\left(\dot{r}_i\cdot\nabla_{r_i}+\dot{p}_i\cdot\nabla_{p_i}\right)\right)F_N=0 \tag{1}$$

where F_N represents the probability density for the system of N particles in the momentum--position space. Figure 1 shows that in the case of gas flow in the specific space for the same initial macroscopic conditions the gas exhibits different trajectories (1, 2 and 3) for each process realization, and this results from the fact that the same macroscopic conditions of the same gas do not correspond to the same microscopic conditions; the initial microscopic states are different and the microscopic states after time t are different as well.

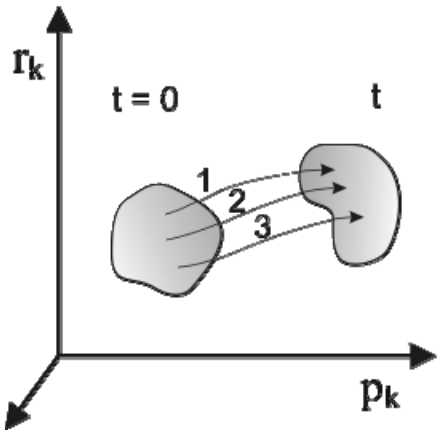

Fig. 1. Trajectories of the phase points

Rys. 1. Trajektorie punktów fazowych

Present form and status of the population balance equation is a result of an application by Hulburt and Katz [3] of the classical Liouville equation to particulate processes and a spectacular success of application of population balancing to modeling and interpretation of crystallization processes [4]. They applied the Liouville equation in so called generic

space, where originally the coordinates are the components of the position and the momentum for any particle, so that the same frame of reference is used for the phase of motion of any particle. When instead of momentum some other coordinates, equivalent to particle properties are applied, then we get the popular form of the population balance equation

$$\frac{\partial n}{\partial t}+\sum_{i=1}^{3}\frac{\partial\left[u_{pi}\left(\vec{x},t\right)n\right]}{\partial x_i}+\sum_{j=1}^{m}\frac{\partial\left[w_{pj}\left(\vec{x},t\right)n\right]}{\partial x_j}=B\left(\vec{x},t\right)-D\left(\vec{x},t\right) \tag{2}$$

where n is the population number density, u_{pi} refers to the component of the rate of change of particle position in the physical space, and w_{pi} refers to the component of rate of change of the particle property, and B and D are the birth and death functions at the point in the phase space. When particle properties are limited to two components: particle mass, m, and particle size, L, then the trajectory in the phase space looks as shown in Fig. 2.

Most often the property of the particle is identified with the particle size, L, and then the population balance equation takes the form

$$\frac{\partial n}{\partial t}+\sum_{i=1}^{3}\frac{\partial\left[u_{pi}\left(\vec{x},t\right)n\right]}{\partial x_i}+\frac{\partial\left[G\left(\vec{x},t\right)n\right]}{\partial L}=B\left(\vec{x},t\right)-D\left(\vec{x},t\right) \tag{3}$$

Considering Fig. 1 we see that the n variable represents in fact a realization average, which mens that there can be a closure problem, especially when the interactions occur between particles. As shown by Ramkrishna [5], this kind of closure problem is important only in the case of small populations, which hardly happens in the case of technical applications.

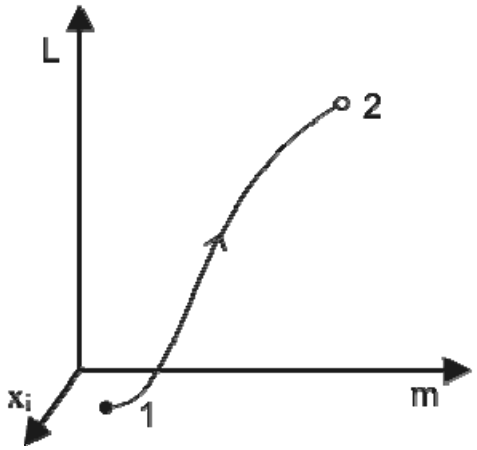

Fig. 2. Trajectory in the phase space in the case of growing particle

Rys. 2. Trajektoria w przestrzeni fazowej ilustrująca wzrost masy i rozmiarów przemieszczającej się cząstki

Equation (3) should be solved together with the mass, momentum, energy and species balances to determine particle velocity in physical space as well as rates of changing of particle properties (in Fig. 2 the rates of mass and size increase). This creates numerical difficulties because the population balance equation should be solved in (m+1)-dimensional space (m is a number of properties here), whereas all other equations are defined in the 3--dimensional physical space. This reduces the number of coordinates to m.

To reduce the dimensionality one can use the volume averaged population balance by using either mechanistic model of micromixing, which enables to take into account not perfect mixing in the system [6], or any other macroscopic domain including the entire equipment, for example the crystallizer [4]. Another method to reduce dimensionality is based on moment transformation of the population balance equation, which reduces the number of coordinates to 3. When aggregation term and the breakage term (size dependent) are included and the growth kinetics is size dependent then the moment equation will be unclosed

$$\frac{\partial m_j}{\partial t} + \sum_{i=1}^{3} \frac{\partial \left(u_{pi}\, m_j \right)}{\partial x_i} = 0^j\, R_N - \int_0^\infty L^j \frac{\partial}{\partial L}\left(Gn \right) dL + \overline{B_{fj}} - \overline{D_{fj}} \tag{4}$$

where $m_j\left(\vec{x}, L, t\right) = \int_0^\infty n\left(\vec{x}, L, t\right) L^j\, dL$ defines the j-th moment of the distribution.

This closure problem can be solved by approximating the distribution by combination of Dirac-delta functions with values of weights and abscissas varying with variation of distribution in such a way that the approximated distribution yields the same moments. The method that can be used for this purpose, called the quadrature method of moments (QMOM), was proposed by McGraw [7], and applied to solve chemical engineering problems see foe example our previous publication [8].

The processes applied in industry have usually turbulent character and modelling of turbulence, that is based very often on Reynolds averaging, leads to closure problems typical for turbulence. This means that there are unclosed terms in the averaged equation

$$\frac{\partial \left\langle m_j \right\rangle}{\partial t} + \sum_{i=1}^{3} \frac{\partial \left\langle u_{pi}\, m_j \right\rangle}{\partial x_i} = 0^j \left\langle R_N \right\rangle + j \left\langle G\, m_{j-1} \right\rangle + \left\langle B_f \right\rangle - \left\langle D_f \right\rangle \tag{5}$$

and they can be modelled using the PDF approach as shown by Bałdyga and Orciuch [9].

Finally the last and most interesting problem results from the fact that the properties of suspension such as the structure of aggregated particles, concentration of particles, the size distribution of primary and aggregated particles affect significantly suspension rheology and details of the flow. Numerical simulations of such flows are difficult because the problem is three-dimensional and time-dependent. The problem is interesting from the scientific point of view because of strong non-linear coupling between suspension structure and the flow. It has practical aspects resulting from industrial relevance of many materials consisting of primary nano-particles that form nano- and micro-aggregates.

2. Method of modelling

2.1. Structure of aggregates

To solve the problem of relation between suspension structure and rheology we represent in what follows the aggregate structure using the concept of fractal geometry; for aggregates of the average size R made up of N building blocks (primary particles) of radius R_0 one can relate the true volume fraction of the primary particles, φ_0, to the effective volume fraction of agglomerates, φ, by

$$\varphi_{eff} = \varphi_0 N^{\frac{3-D_f}{D_f}} = \varphi_0 \left(\frac{R}{R_0} \right)^{3-D_f} \tag{6}$$

where D_f is the fractal dimension of the aggregates.
Equation (6) shows that for fractal aggregates the effective volume fraction that directly affects suspension viscosity can be much larger than the volume fraction of primary particles, φ_o. In the case of processes of industrial importance, often the bifractal or cluster-fractal structure of agglomerates has to be considered to describe properly details of the process.

2.2. Suspension viscosity

In the subject literature one can find many empirical or semi-empirical relations that allow to predict effective viscosity of suspensions. In this work we focus on dense suspensions of nano-aggregates. Typical equation of this type was proposed by Krieger and Dougherty [10]

$$\mu = \mu_{\text{liguid}} \left[1 - \frac{\varphi}{\varphi^*} \right]^{-2,5\varphi^*} \tag{7}$$

Notice that this equation shows just dependence of viscosity on particle volume fraction and neglects dependence on particle size and mechanism creating viscosity (Brownian or shear induced). This is too simple and not useful for our purpose. Hence, we consider and apply in computations relations of another type, valid for both low and high volume fraction of particles, taking into account particle size, and covering the whole range of shear rate values in the flow.
For the concentrated suspension the Pèclet number can be expressed by

$$\text{Pe} = \frac{\dot{\gamma} \cdot a^2}{D_B(\phi)} \tag{8}$$

where

$$D_B(\varphi) = \frac{D_B^{\infty}}{\chi(\varphi)} \tag{9}$$

and

$$D_B^{\infty} = \frac{k \cdot T}{6 \cdot \pi \cdot \mu_{\text{liquid}} \cdot a} \tag{10}$$

where $\chi(\varphi)$ represents effect of particle concentration on Brownian self-diffusion. Buyevich and Kapbsov [11] considered the flows with strong effects of Brownian diffusion ($\text{Pe} \to 0$) and negligible effects of Brownian diffusion ($\text{Pe} \to \infty$), to formulate the relation valid for intermediate Pe values. They denoted the relative viscosity by

$$M(\varphi) = \frac{\mu}{\mu_{\text{liquid}}} \tag{11}$$

and proposed the following relation for the narrow concentration range that adjoins φ^*, the close-packed limit for φ

$$M(\varphi) = -C \cdot \ln\left(1 - \frac{\varphi^{1/3}}{(\varphi^*)^{1/3}}\right) \tag{12}$$

$$C = \frac{z \cdot \varphi^*}{2} \tag{13}$$

where z is an effective „coordination number" of a sphere in the close-packed state. Using equations (12) together with the empirical formula by Frankel and Akrivos [12], that is valid for low and moderate concentrations

$$\mu = \mu_{\text{liquid}} \cdot (1 - \varphi)^{-5/2} \tag{14}$$

Buyevich and Kapbsov [11] developed expression covering whole range of concentrations

$$M_{\infty}(\varphi) = (1 - \varphi)^{-5/2} - C\left\{\ln\left[1 - \left(\frac{\varphi}{\varphi^*}\right)^{1/3}\right] + \sum_{j=1}^{6} \frac{1}{j}\left(\frac{\varphi}{\varphi^*}\right)^{j/3}\right\} \tag{15}$$

with $C \approx 2$, valid at high shear rates, $\text{Pe} \to \infty$

$$M_0(\varphi) = (1 - \varphi)^{-5/2} + 1{,}3 \cdot \left[\left(1 - \frac{\varphi}{\varphi^*}\right)^{-2} - \sum_{j=0}^{2} (1 + j) \cdot \left(\frac{\varphi}{\varphi^*}\right)^{j}\right] \tag{16}$$

valid at low shear rates, $\text{Pe} \to 0$.
For intermediate Pe values the following equation can be used for the whole φ and Pe values

$$M = \frac{M_0 + M_{\infty} \cdot \text{Pe}}{1 + \text{Pe}} \tag{17}$$

Figure 3 shows a range of variation of the relative viscosity for two values of the fractal dimension.

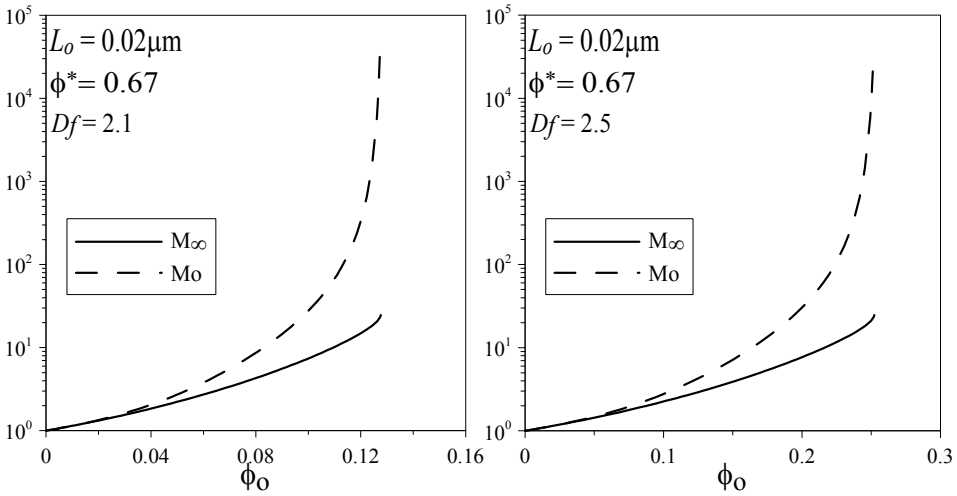

Fig. 3. Predictions of the model by Buyevich and Kabpsov [11]

Rys. 3. Przewidywania modelu Buyevicha i Kabpsova [11]

2.3. Population balance modeling

Hydrodynamic shear induced during the flow affects the aggregate properties (size distribution, structure); on the other hand the rheological properties of aggregated concentrated suspensions depend on the suspension structure, which means that there can be some strong coupling between the structure of suspension and the flow structure. Modeling presented in what follows requires application of the aggregate structure model (fractal), as well as mass and momentum balances (CFD is used here) coupled with population balances (QMOM is applied), and constitutive rheological equations as presented in section 2.2. The time dependent population balance equations are formulated in the three-dimensional physical space using either the aggregate mass or aggregate size as an internal property coordinate, because the size and mass of aggregates are connected to each other by the fractal dimension. Because an average number of primary particles building an agglomerate of mass m_i is equal to

$$N_i = \frac{m_i}{\rho_p V_0} = \frac{m_i}{m_0} \tag{18}$$

one gets relation between the size and mass of an aggregate an a form

$$R_i = R_0 \left(\frac{m_i}{m_0} \right)^{1/D_f} = \frac{L_i}{2} \tag{19}$$

To solve the population balance equation in the CFD environment (Fluent 6.2) with the quadrature method of moments (QMOM) [7], we use n = 3 or 4, with $2n$ = 6 or 8 moments

from which we get $n = 3$ or 4 abscissas m_i and $n = 3$ or 4 weights w_i. Number of abscissas depends on complexity of the density functions, and obviously a bimodality of distribution calls for $n = 4$. Regarding aggregate structure, the local instantaneous values of the average fractal dimension are used in computations; they characterize all aggregates present at certain time at given point in the physical space. The local value of effective volume fraction can be then calculated from

$$\varphi_{eff} = \varphi_0 \sum_{i=1}^{n} N_i^{\frac{3-D_f}{D_f}} \tag{20}$$

to be used in viscosity calculations.

To model aggregation processes we use in the case of laminar flow the classical relations by Smoluchowski [2] for the peri- and the orthokinetic aggregation regimes. We assume that superposition of both mechanisms is possible as shown in Eq.(21) and discussed by Friedlander [13]; other more complex kernels, that for example take into account effects of colloidal forces [14], can be used in modeling as well, without computational problems

$$\beta_{ij} = 4\pi D_{ij}^{\infty}\left(\frac{L_i}{2}+\frac{L_j}{2}\right)+\frac{4}{3}\dot{\gamma}\left(\frac{L_i}{2}+\frac{L_j}{2}\right)^3 \tag{21}$$

In the case of turbulent flow the k-ε and the large eddy simulations (LES) models, both by Fluent, are applied. In the case of k-ε model the Smoluchowski's orthokinetic kernel is replaced by Saffman and Turner [15] kernel, which is almost identical, however, with the rate of strain expressed using Kolmogorov theory of turbulence, $\dot{\gamma} = (\varepsilon/\nu)^{1/2}$, and 1,3 instead of 4/3 for the proportionality constant. In the case of LES we recalculate the rate of strain $\dot{\gamma}$ from the resolved rate of strain $\dot{\gamma}_r$ using the model by Smagorinsky; from the expression on the dissipation rate $\varepsilon = (\dot{\gamma})_r^2 (\nu + \nu_e)$ we see that the subgrid dissipation rate reads $\varepsilon' = (\dot{\gamma})_r^2 \nu_e$, and

$$\dot{\gamma} = (\dot{\gamma})_r + \left(\frac{\varepsilon'}{\nu}\right)^{1/2} = \dot{\gamma}_r\left[1+\left(\frac{\nu_e}{\nu}\right)^{1/2}\right] \tag{22}$$

where the eddy viscosity is calculated from the Smagorinsky model

$$\nu_e = l^2\sqrt{\left(\frac{\partial u_i}{\partial x_j}+\frac{\partial u_j}{\partial x_i}\right)\left(\frac{\partial u_i}{\partial x_j}+\frac{\partial u_j}{\partial x_i}\right)} \tag{23}$$

with $l = (\Delta_1 \cdot \Delta_2 \cdot \Delta_3)^{1/3}$ being the mixing length, and Δ_1, Δ_2 and Δ_3 representing grid mesh size in directions 1, 2 and 3.

The model of breakage that is applied in the population balance equations is based on the comparison of the tensile strength of aggregates with the hydrodynamic stress generated by the flow and acting on aggregates. The aggregate mechanical strength depends on the inter-particle forces i.e. forces of interaction between the primary particles building the fractal particle (aggregate). In the breakage model the agglomerate tensile strength is

compared with hydrodynamic stress, and if the rupture force exceeds the aggregate durability the break up process should occur with characteristic frequency proportional to the local value of shear rate $\dot{\gamma}$. Otherwise the aggregate is strong enough to resist the stresses and the local rate of break up is set to zero. The tensile strength of aggregates can be expressed using the relation proposed by Tang et al. [15]

$$\sigma_T = 1{,}1 \cdot \frac{(1-\varepsilon)}{\varepsilon} \cdot \frac{F}{L_0^{\,2}} \tag{24}$$

where F is the bonding force between primary particles an ε represents here porosity of aggregates that is obviously related to effective volume of an aggregate, Eq.(6).
The resulting force of interaction between primary particles in an aggregate can be calculated as the sum of van der Waals attractive and electrostatic repulsive forces as proposed in [15].
Comparing tensile strength of aggregates with hydrodynamic stresses and taking into account characteristic hydrodynamic frequency one gets relations for the breakage kernel; for example in the case of laminar flow

$$\begin{cases} \Gamma = C_b \cdot \dot{\gamma} & \text{if} \quad \mu \cdot \dot{\gamma} > \sigma_T \\ \Gamma = 0 & \text{if} \quad \mu \cdot \dot{\gamma} \le \sigma_T \end{cases} \tag{25}$$

In the case of turbulent flow for aggregates smaller than the Kolmogorov microscale, $\lambda_K = \left(\nu^3/\varepsilon\right)^{1/4}$, Eq. (25) works with properly defined deformation rate, $\dot{\gamma}$, as discussed above. For turbulent flows, and for aggregates larger than the Kolmogorov microscale, $L > \lambda_k$

$$\begin{cases} \Gamma = C_b \cdot \dfrac{\varepsilon^{1/3}}{L^{2/3}} & \text{if} \quad \rho \cdot \varepsilon^{2/3} \cdot L^{2/3} > \sigma_T \\ \Gamma = 0 & \text{if} \quad \rho \cdot \varepsilon^{2/3} \cdot L^{2/3} \le \sigma_T \end{cases} \tag{26}$$

where C_b is a proportionality constant.

During the flow aggregates change their structure, which in our case is expressed by variation of the aggregate size and its fractal dimension. There are three mechanisms which affect the restructuring process, namely shear, aggregation and breakage. The effect of each of these mechanisms is different and one can treat them as occurring simultaneously. Hence, to calculate the overall change of fractal dimension we assume superposition of three mechanisms. Shear stress (without breakage) tends to make the structure of aggregates more compact, and thus the fractal dimension increases. The influence of aggregation is opposite, and the applied limiting lowest value of the fractal dimension for this mechanism is assumed to be $D_{f,\mathrm{agg}}$ = 1,8, which corresponds to fractal dimension for cluster-cluster agglomeration, as explained for example in the book by Friedlander [13]. Fractal dimension thus decreases due to agglomeration events. On the other hand when the aggregate breaks and one assumes that the internal porosity is conserved, then the fractal dimension of two secondary agglomerates (equal to each other in an example presented below) must be different than that of the primary aggregate. From relation

$$\left(\frac{R}{R_0}\right)^{D_f} = 2\cdot\left(\frac{R/2^{1/3}}{R_0}\right)^{D_{f,\mathrm{break(min)}}} \tag{27}$$

one gets

$$D_{f,\mathrm{break(min)}} = 3\cdot\frac{D_f\cdot\ln\left(R/R_0\right)-\ln(2)}{3\cdot\ln\left(R/2\cdot R_0\right)+2\cdot\ln(2)} \tag{28}$$

and Eq.(28) represents relaxation limit for restructuring due to the breakage. The evolution equation for fractal dimension, treating variation of the fractal dimension as relaxation, can be thus written as

$$\frac{DD_f}{Dt} = C_{\mathrm{shear}}\gamma\left(D_{f,\mathrm{shear(max)}}-D_f\right)+C_{\mathrm{agg}}\beta\left(D_{f,\mathrm{agg(min)}}-D_f\right)+C_{\mathrm{break}}\Gamma\left(D_{f,\mathrm{break(min)}}-D_f\right) \tag{29}$$

which represents extension of the approach proposed by Selomulya et al. [16].

3. Results and discusson

We start from presenting results of computations illustrating abilities and properties of the model. Hence, the first three figures in this section illustrate application of population balance to the aggregation-breakage-restructuring process carried out in the one--dimensional system (plug flow system or butch mixer). Presented results are for Hamaker constant equal to 10^{-21} J, rate of energy dissipation equal to $\varepsilon = 10^5\ m^2/s^3$ and initial value of fractal dimension equal to 2,85. Figures 4, 5 and 6 show time variation of average sizes of aggregates, $L_{ij} = m_i/m_j$, fractal dimension, effective viscosity and effective volume fraction of aggregates.

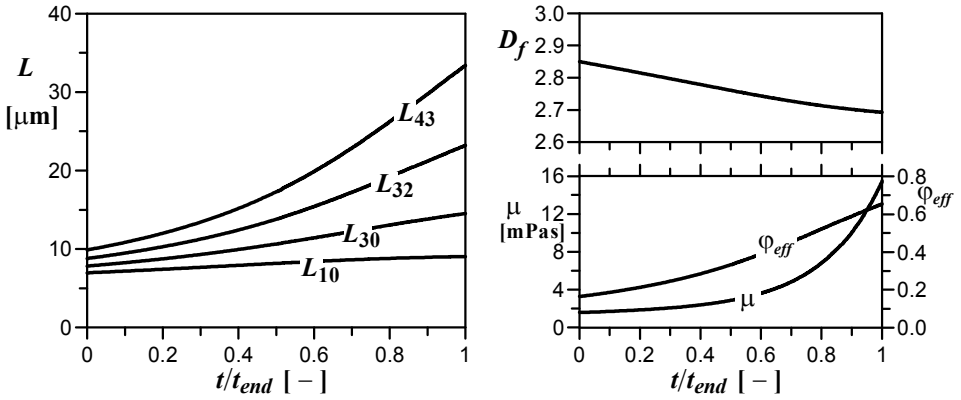

Fig. 4. Progress of aggregation–breakage–restructuring process illustrating dominating effect of aggregation

Rys. 4. Przebieg procesu agregacji–rozpadu–restrukturyzacji agregatów; ilustracja dominującego efektu agregacji

Figure 4 shows the process dominated by aggregation. Aggregation decreases the fractal dimension of aggregates, increases aggregate volume fraction and increases viscosity of suspension. In the case of stabilized suspension aggregation is blocked and breakage dominates the process, which results in decrease of the aggregate size and decreases effective viscosity of suspension as well (Fig. 5). Finally Fig. 6 shows pure effect of restructuring; obviously in this case aggregates become more compact and smaller, which decreases the effective viscosity as well.

Presented results illustrate universality and flexibility of population balance modeling. In what follows presented above population balance method will be linked to CFD.

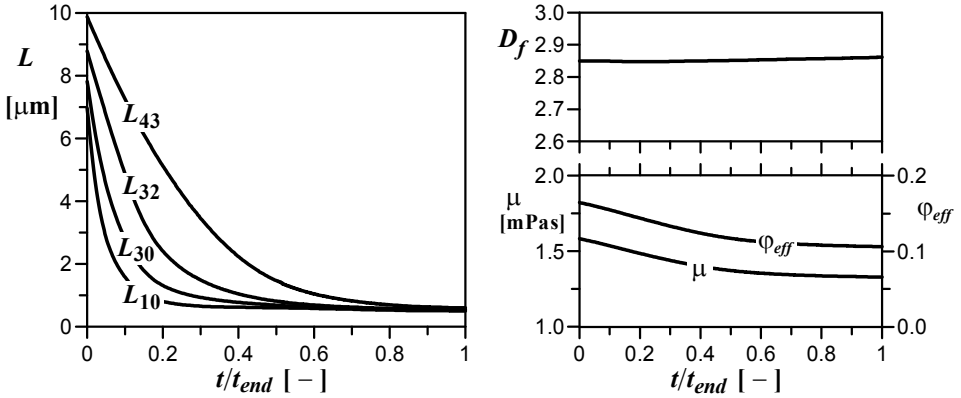

Fig. 5. Progress of breakage-restructuring process for stabilized dispersion illustrating dominating effect of breakage

Rys. 5. Przebieg procesu agregacji - rozpadu - restrukturyzacji agregatów; ilustracja dominującego efektu rozpadu w przypadku stabilizacji zawiesiny

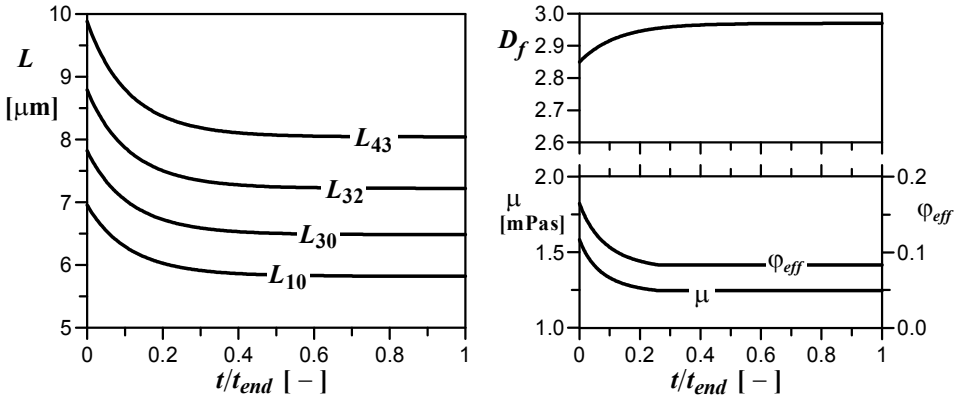

Fig. 6. Progress of restructuring process

Rys. 6. Przebieg procesu restrukturyzacji agregatów

To illustrate application of LES method application we consider the flow and deaggregation in equipment applied by Dąbroś and van de Ven [17].

The LES (*Large Eddy Simulation*) method was applied in simulation for the system geometry presented in Fig. 7. The contours of properties of the flow and suspension (velocity, viscosity, volume fraction of the solid etc.) are shown in Fig. 8. One can observe that changes of nano-aggregates structure and subsequent viscosity changes proceed very fast as the suspension flows through the gap (nozzle), where the strain rate reaches the highest values. The impact of fluid into the wall behind the nozzle and also some shear effects close to the wall strongly affect the suspension structure properties and observed viscosity. LES are able to predict both laminar flow at the inflow to the system, local intensive turbulence close to the nozzle as well as the flow laminarization at the outflow.

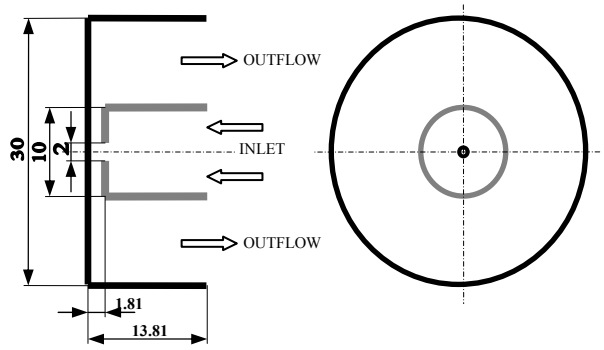

Fig. 7. Geometry of the system for simulating the axisymmetrical extensional flow (described in detail in work of Dąbroś and van de Ven [17])

Rys. 7. Schemat układu do symulacji osiowo-symetrycznego przepływu rozciągającego (szczegóły w pracy Dąbrosia i van de Vena [17])

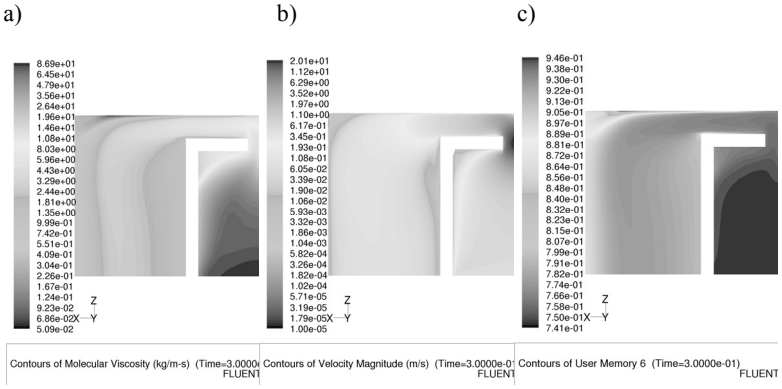

Fig. 8. Results of computation for LES: $\varphi_0 = 0{,}139$, D_f(inlet) = 2,6, u(inlet) = 0,5 m/s; a) effective viscosity of suspension [Pa·s], b) velocity [m/s], c) effective volume fraction

Rys. 8. Wyniki symulacji z użyciem metody LES: $\varphi_0 = 0{,}139$, D_f(wlot) = 2,6, u(wlot) = 0,5 m/s; a) lepkość efektywna [Pa·s], b) prędkość [m/s], c) efektywny ułamek objętości

Presented method of modeling has been used to interpret deagglomeration processes in systems of industrial importance using the *k*-ε model of turbulence [8, 18] and the multiple reference frame. Because in the case of typical industrial equipment, the rotor-stator system, deagglomeration effects for one passage through the mixer are very small, thus in practical applications the suspension circulates many times through the mixing head as shown in Fig. 9.

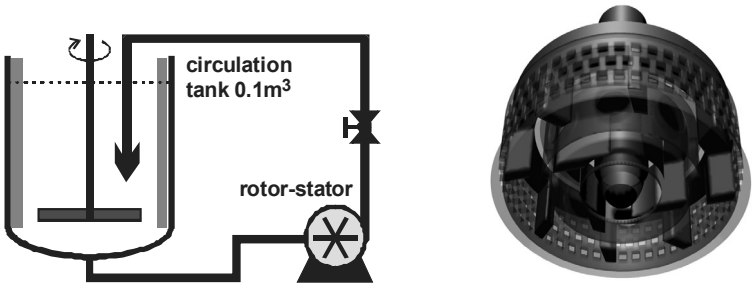

Fig. 9. Schematic of the experimental system and the rotor-stator geometry

Rys. 9. Schemat układu badawczego i geometria mieszalnika typu rotor-stator

Figures 10 and 11 show typical results of simulations. Figure 10 shows the zone of high breakage rate defined here by the breakage kernel values exciding 0,2 s^{-1}. One can see that breakage is obsered within the volume behind external screen with square holes and in jets emerging from these holes. Figure 11 shows changes in the agglomerate size distrbution (Aerosil) during the process for Aerosil concentration equal to 20%. The bimodal size distribution is well predicted.

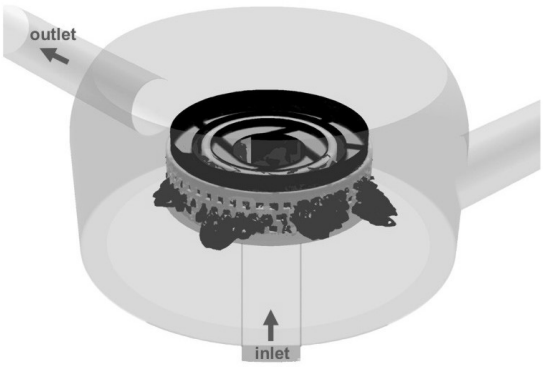

Fig. 10. The zone of particle breakage in the rotor-stator

Rys. 10. Obszar rozpadu agregatów w mieszalniku typu rotor-stator

4. Conclusions

Proposed model combining the flow (CFD), suspension structure (population balance for aggregates forming suspension and fractal structure of aggregates) and the constitutive rheological equations form together a complex model of universal character. The model is flexible and able to simulate breakage, aggregation and restructuring of aggregates as well as predict suspension viscosity. The model can be used to model processes of industrial importance carried out in equipment of complex geometry.

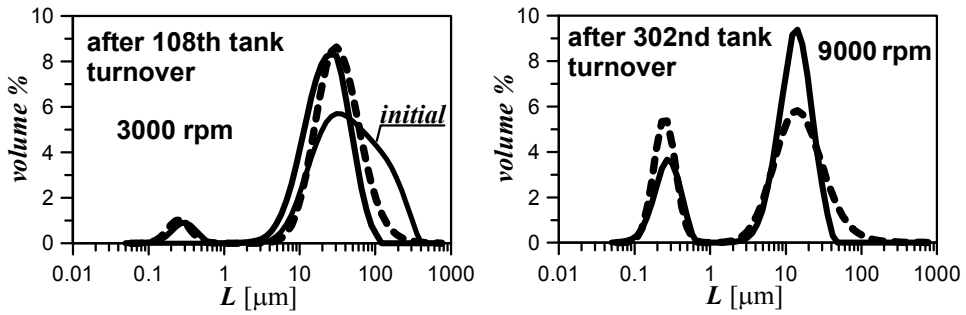

Fig. 11. Progress of deagglomeration in the system shown in Fig. 9. Experimental results [18] are marked by solid lines, and results of simulations by broken lines

Rys. 11. Postęp deaglomeracji w układzie przedstawionym na rys. 9. Wyniki doświadczalne oznaczono linią ciągłą, wyniki symulacji linią przerywaną

References

[1] Gibbs J.: *Elementary Principles in Statisticasl Mechanics*, Yale University Press, 1902 (Dover Publications, New York 1960).
[2] Smoluchowski M.: Z. Phys. Chem., **92**, 1917, 129-168.
[3] Hulburt H. M., and Katz S. L.: Chem. Eng. Sci., **19**, 1964 555-574.
[4] Randolph A.D. and Larson M.A.: *Theory of Particulate Processes*, Academic Press, New York, 1971.
[5] Ramkrishna D.: *Population Balances*, Academic Press, London, 2000.
[6] Bałdyga J., Podgórska W., Pohorecki R.: Chem. Eng. Sci., **50**, 1995, 1281-1300.
[7] McGraw R.: Aerosol Sci. Techn., **27**, 1977, 255-265.
[8] Bałdyga J., Orciuch W., Makowski Ł., Malski-Brodzicki M., Malik K.: Chem. Eng. & Proc., **46**, 2007, 851-861.
[9] Bałdyga J., Henczka M., Orciuch W.: Acta Polytechnica Scandinavica, Chem. Technology Series, **244**, 1977, 41-43.
[10] Krieger I. M., Dougherty T. J.: Trans. Soc. Rheol., **3**, 1959, 137-152.
[11] Buyevich Yu. A., Kapbsov S.K.: J. Non-Newt. Fluid. Mech., **86**, 1999, 157--184.

[12] Frankel N. A., Akrivos A.: Chem. Eng. Sci., **22**, 1967, 847-853.
[13] Friedlander S. K.: *Smoke, Dust, and Haze. Fundamentals of Aerosol Dynamics*, 2nd Edition, Oxford University Press, New York, 2000.
[14] Bałdyga J., Jasińska M., Orciuch W.: Chem. Eng.Technol., **26**, 2003, 334-340.
[15] Tang S., Ma Y., Shiu C.: *Colloids and Surfaces: A Physical and Engineering Aspects*, **180**, 1987, 7-16.
[16] Selomulya C., Bushell G., Amal R., Waite T. D.: Chem. Eng. Sci., **58**, 2003, 327-338.
[17] Dąbroś T., van de Ven T. G. M.: PCH Phys.-Chem. Hydr., **8**, No. **2**, 1987, 161--172.
[18] Bałdyga J., Orciuch W., Makowski Ł., Malik K., Ozcan-Taskin G., Eagels W., Padron G.: Ind. Eng. Chem. Res., accepted for publication 2008, published on Web 01/08/2008.

This study was carried out within the project PROFORM („Transforming Nano-particles into Sustainable Consumer Products Through Advanced Product and Process Formulation" EC Reference NMP4-CT-2004-505645) which was partially funded by the 6th Framework Programme of EC. The contents of this paper reflects only the authors' view. The authors gratefully acknowledge the useful discussions held with other partners of the Consortium: BHR Group Limited; Karlsruhe University, Institute of Food Process Engineering; Bayer Technology Services GmbH; University of Loughborough; Unilever UK Central Resources Limited; Birmingham University School of Engineering; Poznań University of Technology, Institute of Chemical Technology and Engineering; Rockfield Software Limited; C3M d.o.o. Ljubljana.